

Electronic Supplementary Information

Journal of Materials Chemistry C

Open system massive synthesis of narrow-band blue and green fluorescent graphene quantum dots and their application to water sensing

Yukino Ochi, Ayano Otani, Rika Katakami, Akihiro Ogura, Ken-ichi Takao, Yoshiki Iso^{*}
and Tetsuhiko Isobe^{*}

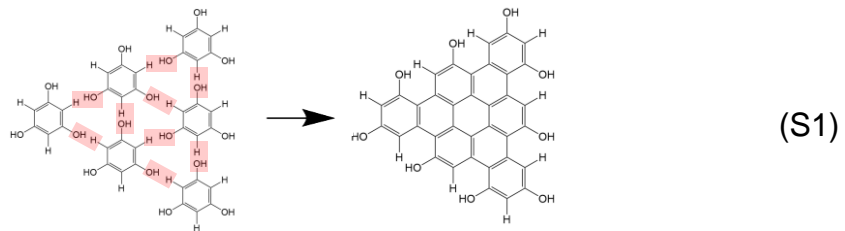
*Department of Applied Chemistry, Faculty of Science and Technology, Keio University,
3-14-1 Hiyoshi, Kohoku-ku, Yokohama 223-8522, Japan*

^{*}Corresponding authors.

Yoshiki Iso – E-mail: iso@aplc.keio.ac.jp; Tel.: +81 45 566 1558; Fax: +81 45 566
1551; orcid.org/0000-0001-7483-2828

Tetsuhiko Isobe – E-mail: isobe@aplc.keio.ac.jp; Tel.: +81 45 566 1554; Fax: +81 45
566 1551; orcid.org/0000-0002-0868-5425

PG-derived GQDs



RS-derived GQDs

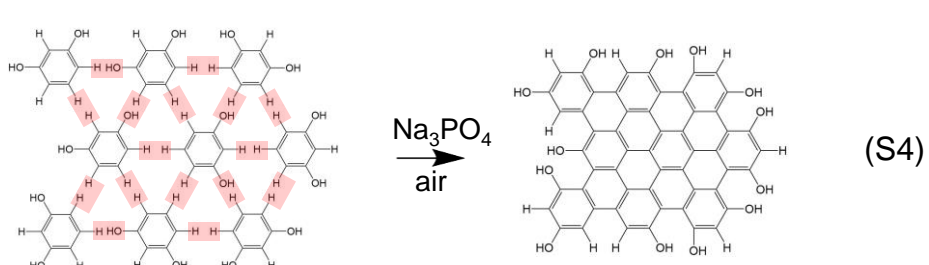
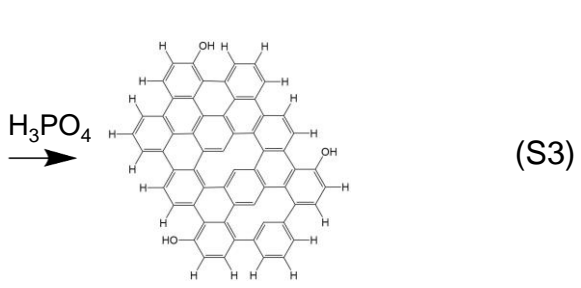
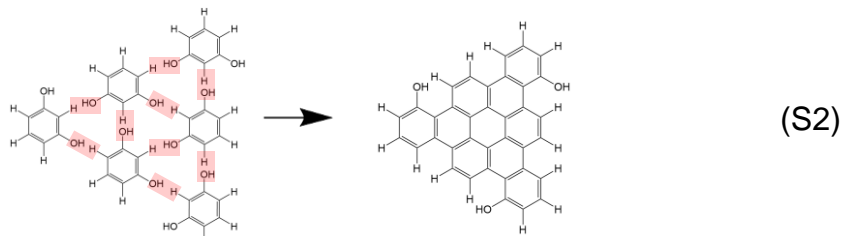


Fig. S1 Formation of GQDs from PG and RS. The solvothermal reactions (S1) and (S2) in ethanol at 200 °C have been reported by Y. L. Yuan et al.^{S1,S2} The reactions (S3) and (S4) in ethylene glycol at 190 °C have been reported by S. Ghosh et al.^{S3}

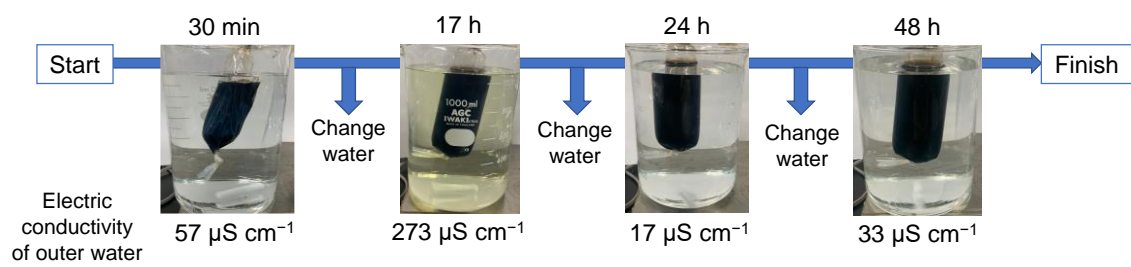


Fig. S2 Purification of PG-GQDs by dialysis.

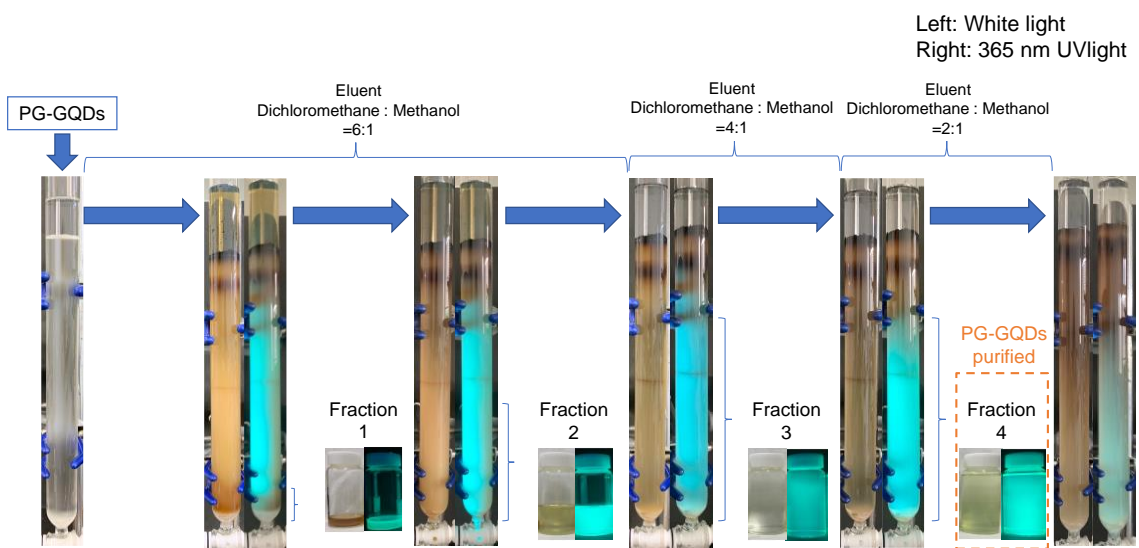


Fig. S3 Purification of PG-GQDs by silica gel column chromatography.

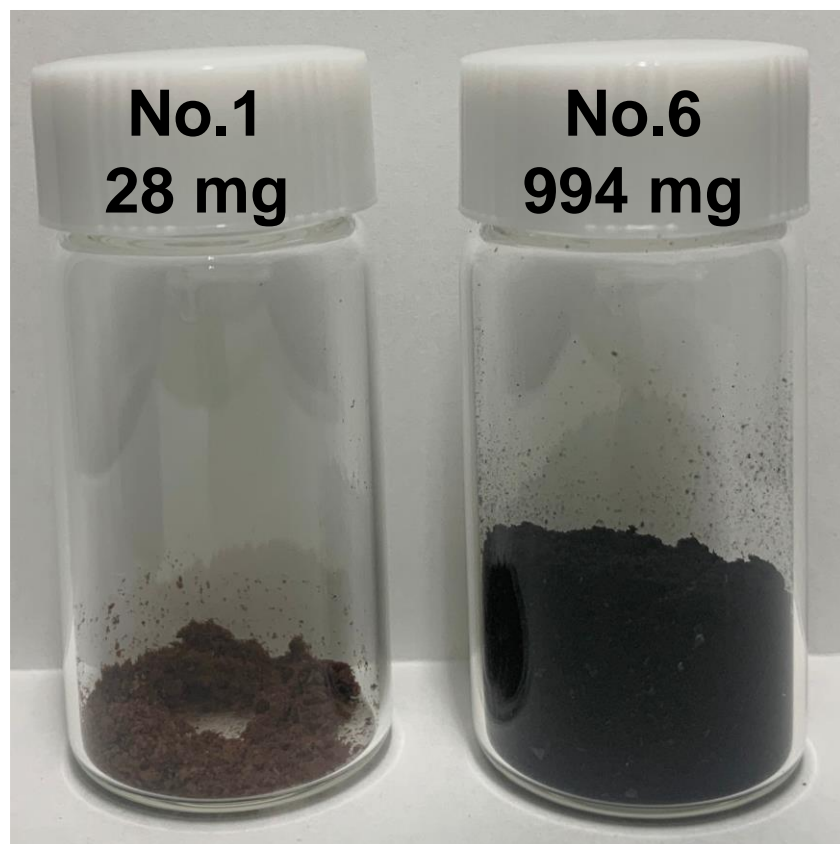


Fig. S4 Photographs of crude PG-GQDs synthesized under the conditions Nos. 1 and 6.

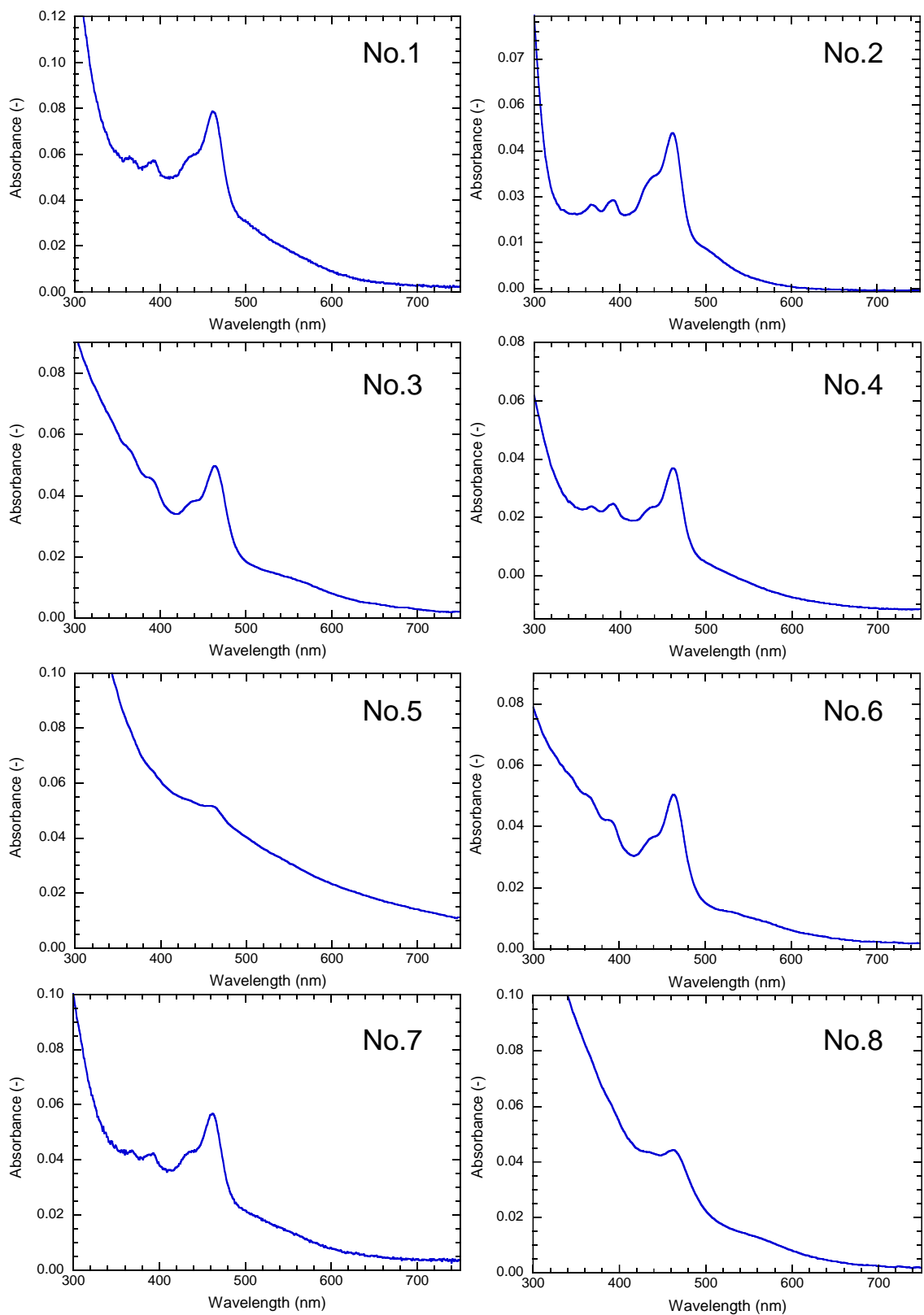


Fig. S5 UV-vis absorption spectra of crude PG-GQDs in EtOH.

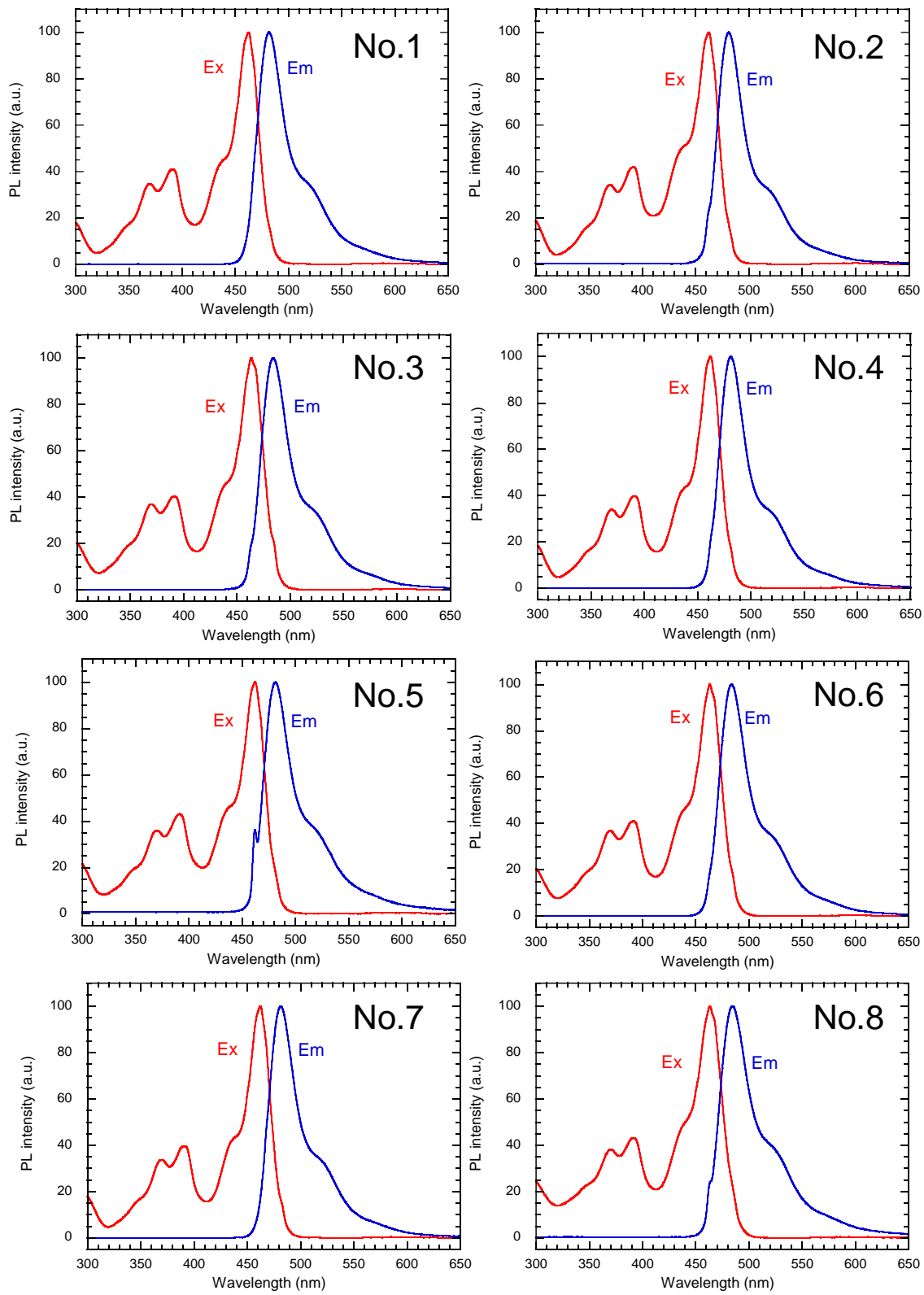


Fig. S6 PL/PLE spectra of crude PG-GQDs in EtOH.

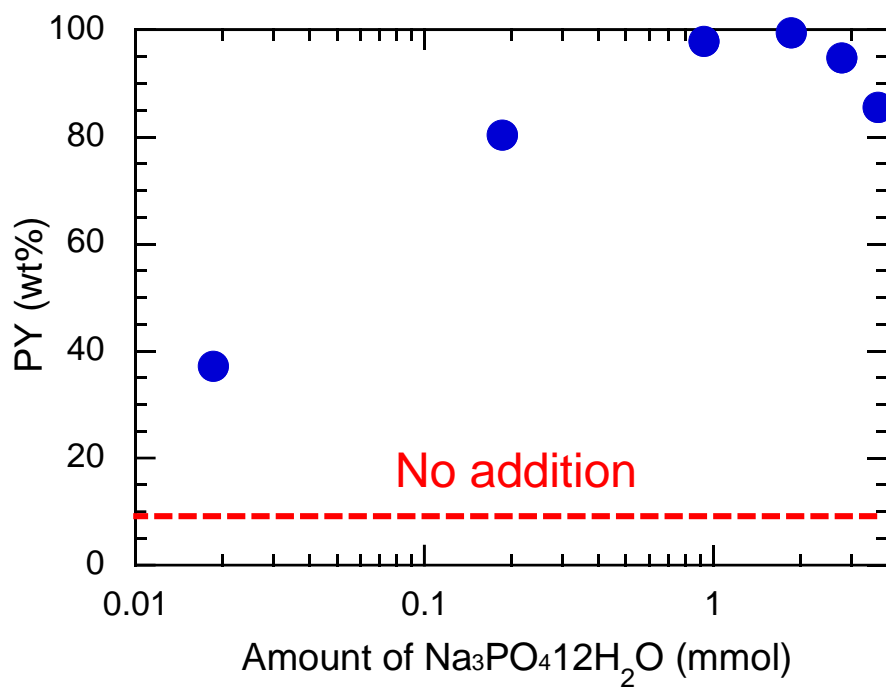


Fig. S7 Change in PY with amount of $\text{Na}_3\text{PO}_4 \cdot 12\text{H}_2\text{O}$ catalyst.

Table S1 Change in PY with amount of $\text{Na}_3\text{PO}_4 \cdot 12\text{H}_2\text{O}$ catalyst.

| Amount of $\text{Na}_3\text{PO}_4 \cdot 12\text{H}_2\text{O}$ (mmol) | PY (wt%) |
|--|----------|
| 0 | 2.8 |
| 0.0186 | 37.2 |
| 0.186 | 80.3 |
| 0.930 | 97.8 |
| 1.86 | 99.4 |
| 2.79 | 94.8 |
| 3.72 | 85.5 |

Table S2 PL properties of three different synthesized and purified PG-GQDs ($\text{Na}_3\text{PO}_4 \cdot 12\text{H}_2\text{O}$, air) in EtOH.

| | λ_{ex} (nm) | λ_{em} (nm) | fw hm (nm) | PLQY (%) |
|---------|----------------------------|----------------------------|------------|----------|
| 1 | 463 | 483 | 32 | 72 |
| 2 | 463 | 484 | 32 | 80 |
| 3 | 464 | 485 | 32 | 73 |
| Average | 463 | 484 | 32 | 75 |

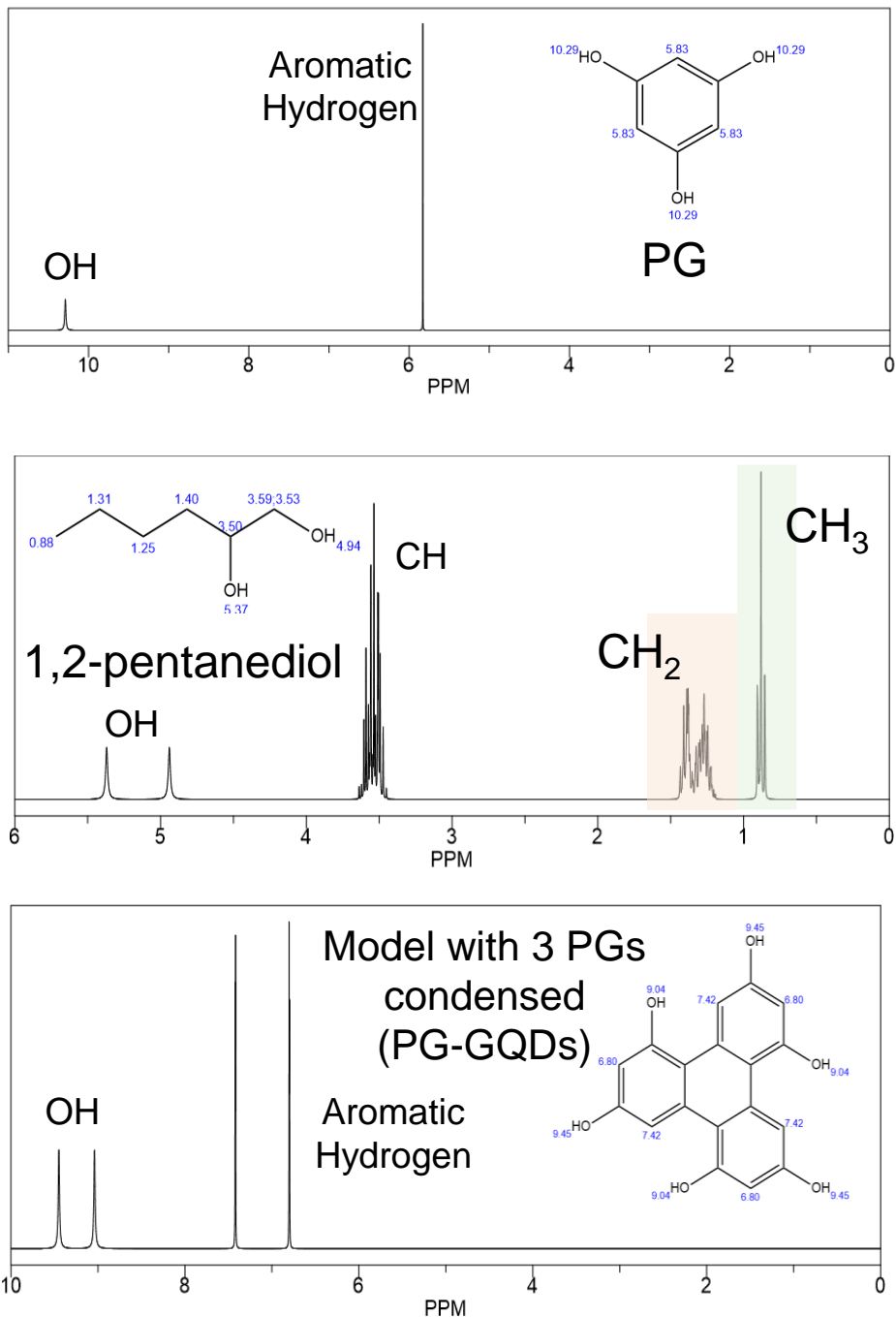


Fig. S8 Simulated ^1H -NMR spectra of PG, 1,2-pentanediol, and the molecule formed by dehydration condensation of three PG molecules.

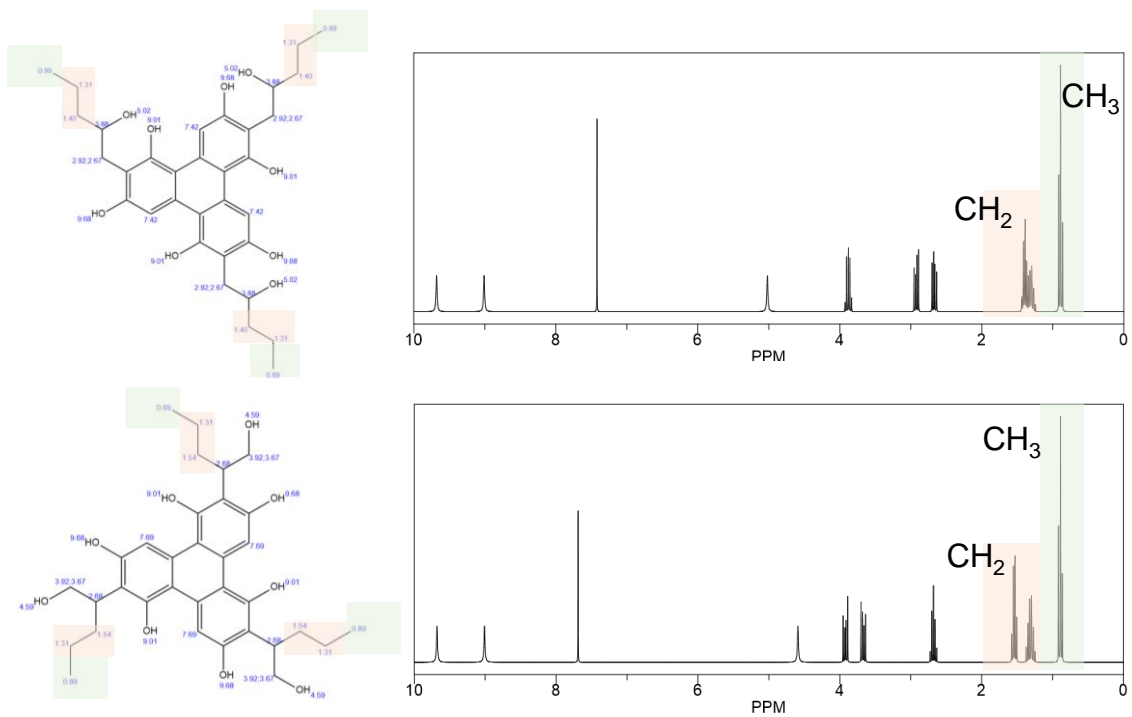


Fig. S9 Simulated ^1H -NMR spectra of the dehydration-condensed structure of three PG molecules bonded to three 1,2-pentanediol molecules.

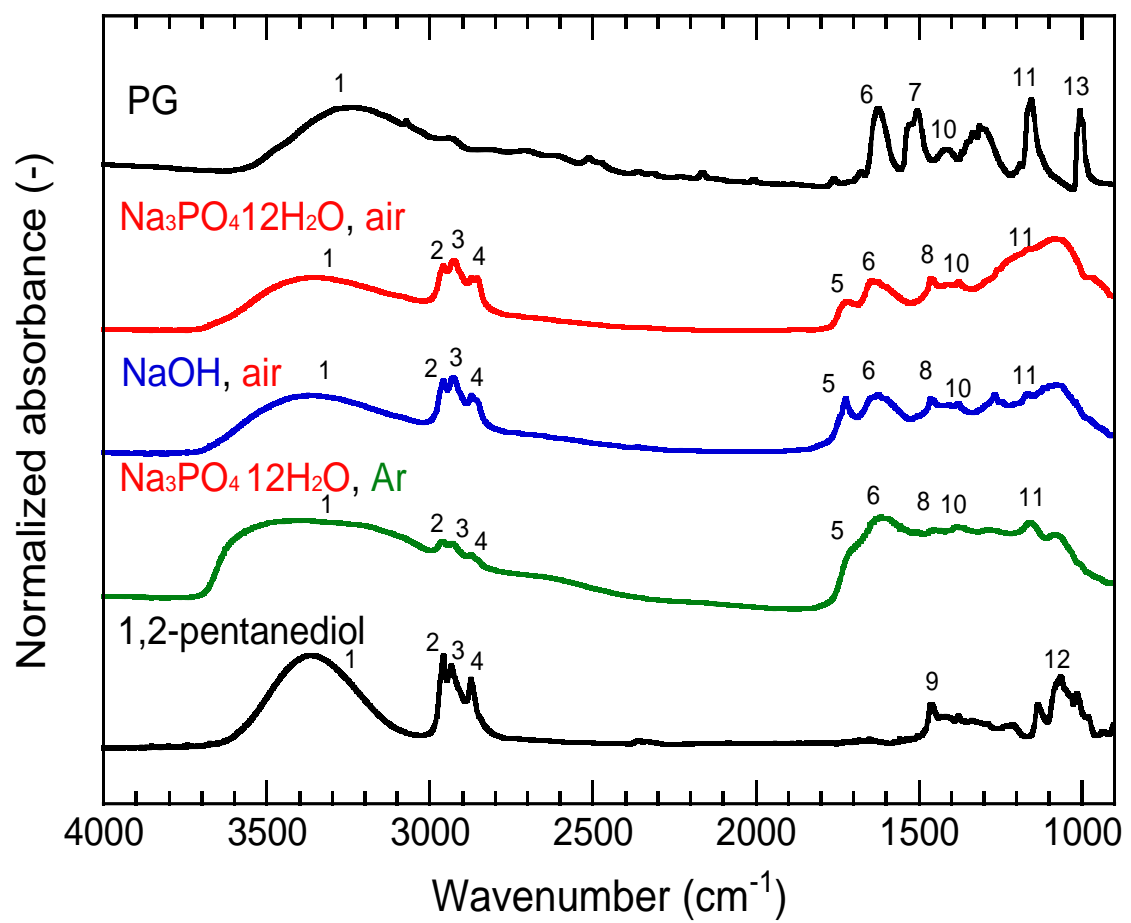


Fig. S10 FT-IR spectra of PG, purified PG-GQDs, and 1,2-pentanediol.

Table S3 Assignments of FT-IR absorption peaks shown in Fig. S10.

| Peak | PG | Wavelength (cm ⁻¹) | | | | Assignment |
|------|---------------|---|-----------|--|---------------------|------------------------------------|
| | | Na ₃ PO ₄ ·12H ₂ O, air | NaOH, air | Na ₃ PO ₄ ·12H ₂ O, Ar | 1,2- pentanediol | |
| 1 | 3100- 3600 | v(O-H) | | | | |
| 2 | | 2959 | 2959 | 2960 | 2959 | v _{as} (CH ₃) |
| 3 | | 2926 | 2929 | 2931 | 2934 | v _s (CH ₃) |
| 4 | | 2873 | 2873 | 2874 | 2873 | v _s (CH ₂) |
| 5 | | 1717 | 1725 | 1704 | | v(C=O) |
| 6 | 1626 | 1645 | 1626 | 1627 | | ring(C=C) ring |
| 7 | 1506 | | | | | semicircle stretching |
| 8 | | 1464 | 1466 | 1464 | | ring semicircle stretching |
| 9 | | | | | 1466 | δ(CH ₂) |
| 10 | 1415 | 1410 | 1409 | 1408 | | δ(O-H) |
| 11 | 1156 | 1162 | 1166 | 1160 | | v(C-O) |
| 12 | | | | | 1066 | v _{as} (C-C-O) |
| 13 | 1008 | | | | | δ(C-H) |

v=stretching, δ=deformation or bending, as=asymmetric, s=symmetric

PG-GQDs RS-GQDs

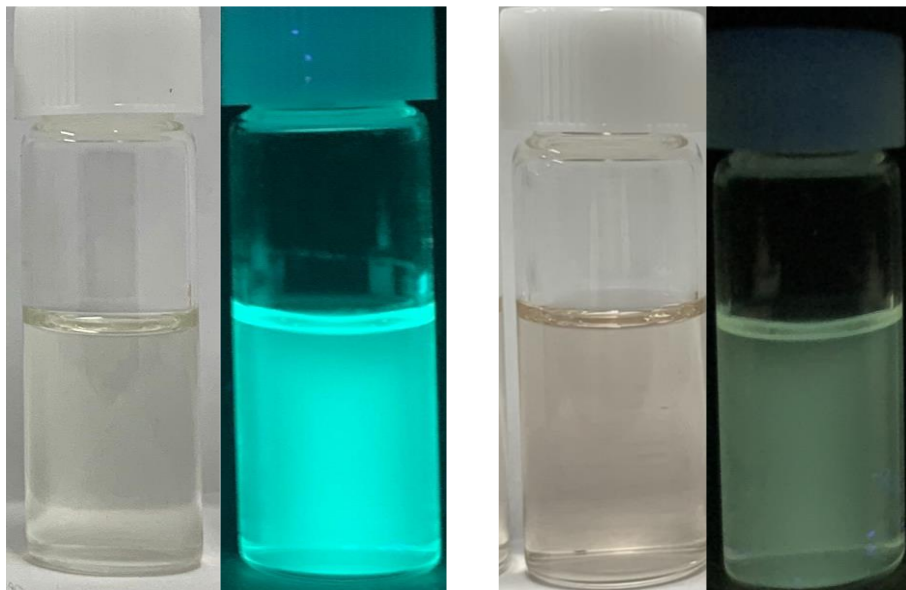


Fig. S11 Photographs of purified PG-GQDs and RS-GQDs in EtOH under white light and 365 nm UV light.

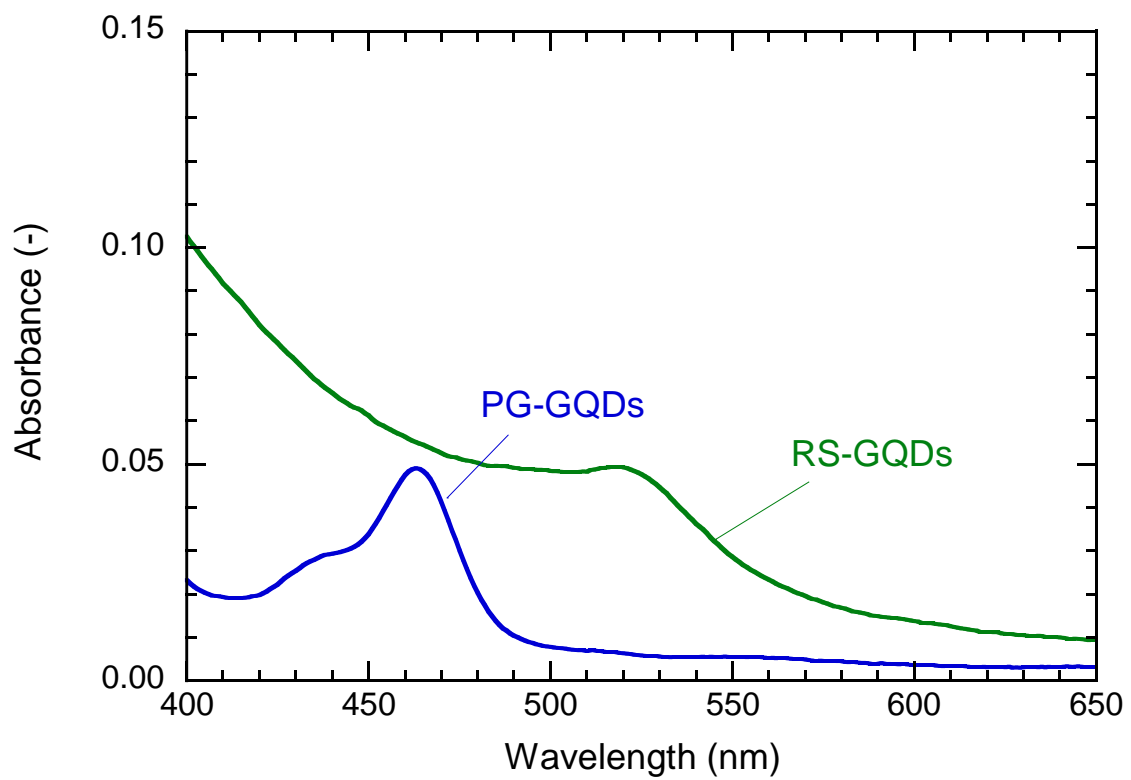


Fig. S12 UV-vis absorption spectra of purified PG-GQDs and RS-GQDs in EtOH.

Table S4 Optical properties of purified PG-GQDs and RS-GQDs in EtOH.

| | Absorption wavelength (nm) | Excitation wavelength (nm) | Emission wavelength (nm) | fwhm (nm) | PLQY (%) |
|---------|----------------------------------|-------------------------------|-----------------------------|--------------|-------------|
| PG-GQDs | 463 | 463 | 483 | 32 | 75 |
| RS-GQDs | 518 | 524 | 542 | 40 | 13 |

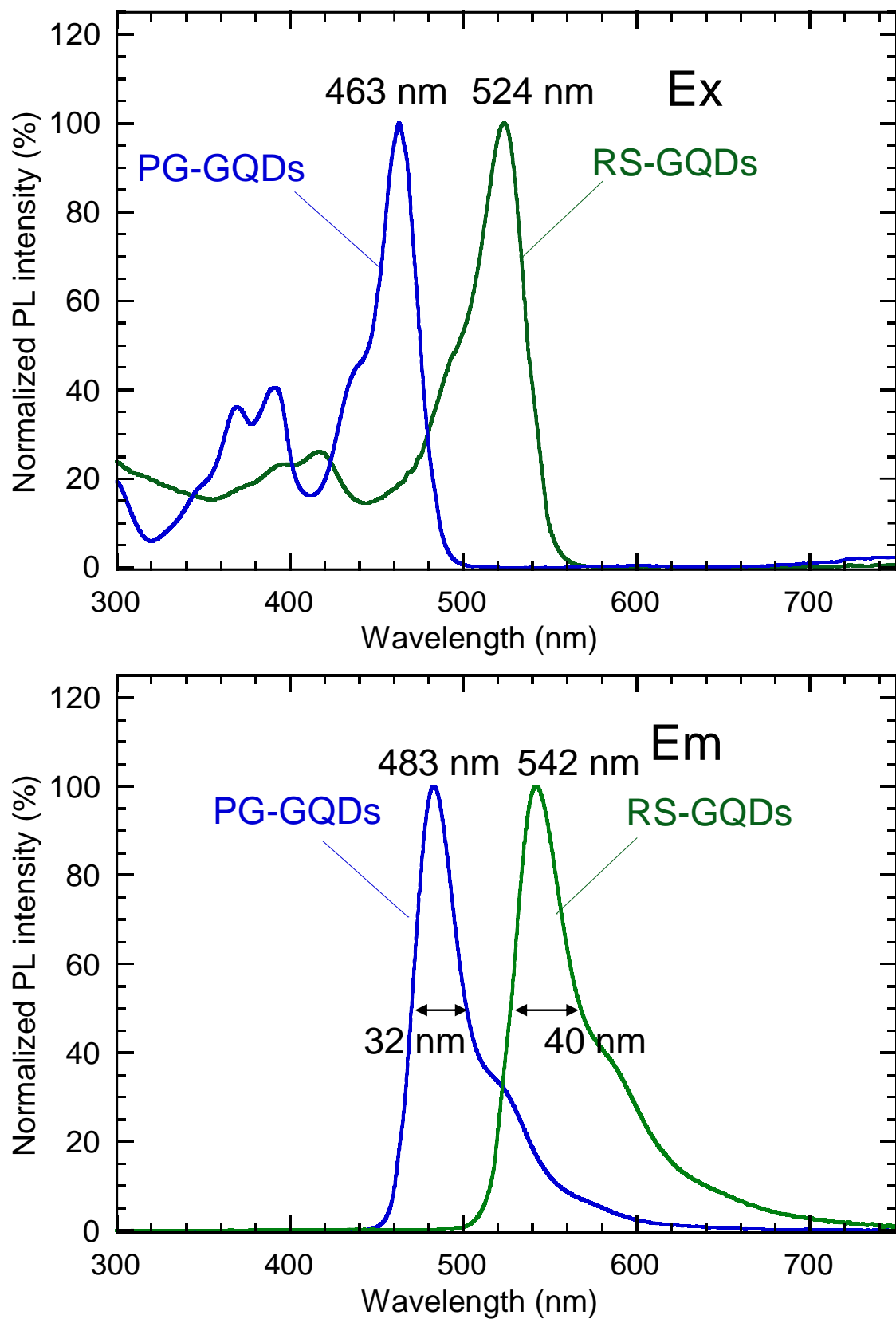


Fig. S13 PL/PLE spectra of purified PG-GQDs and RS-GQDs in EtOH.

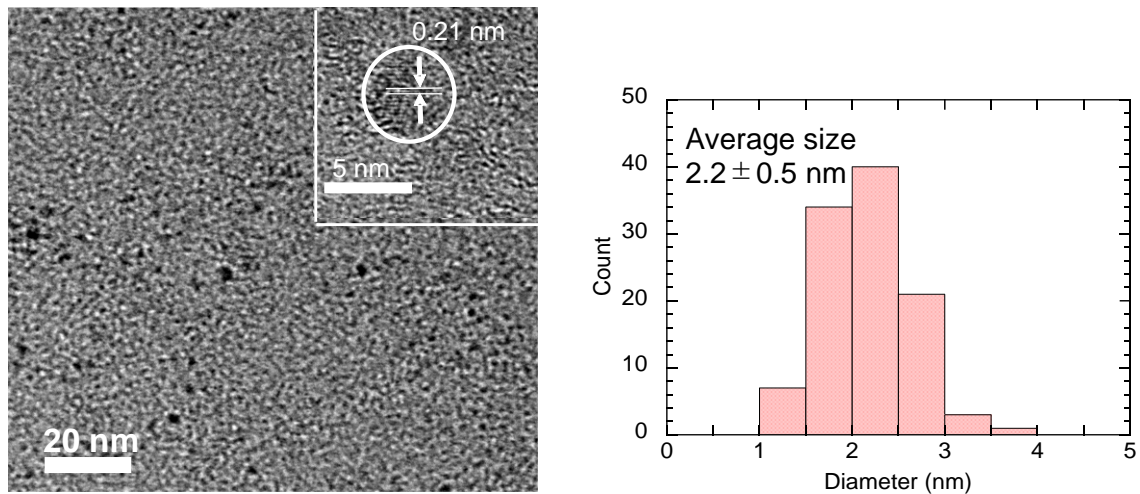


Fig. S14 FE-TEM images of RS-GQDs and their size distribution.

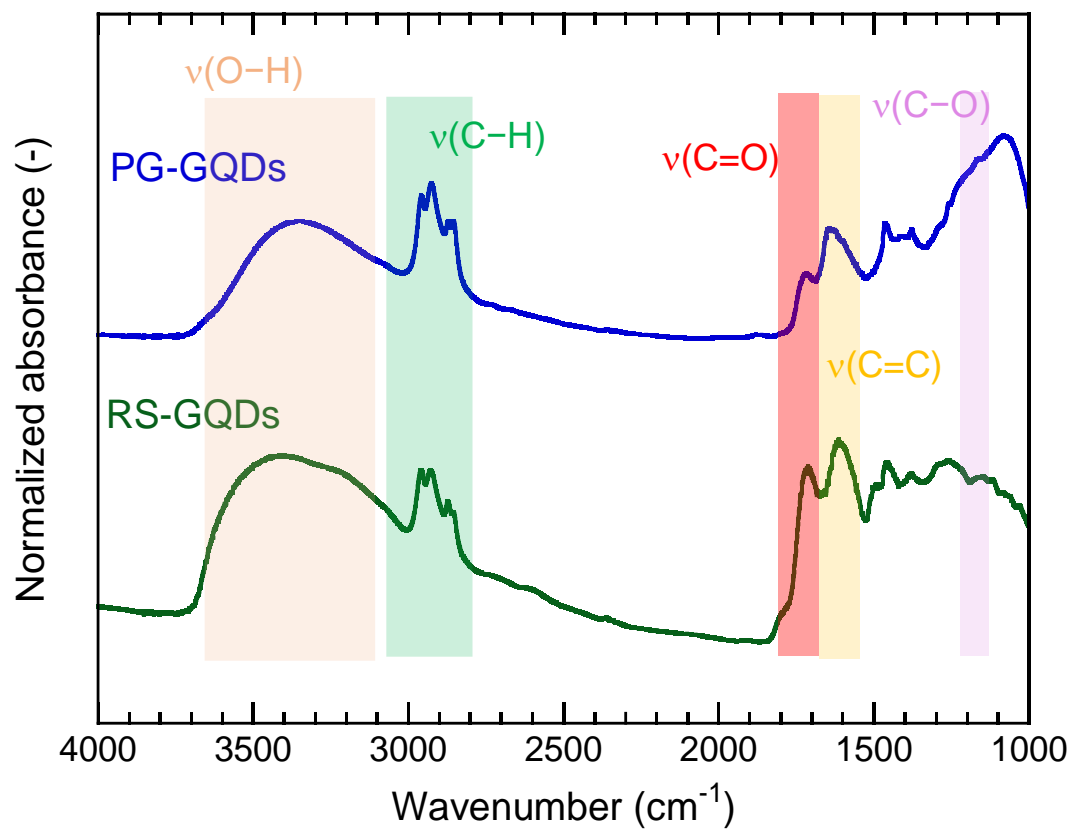


Fig. S15 FT-IR spectra of purified PG-GQDs and RS-GQDs.

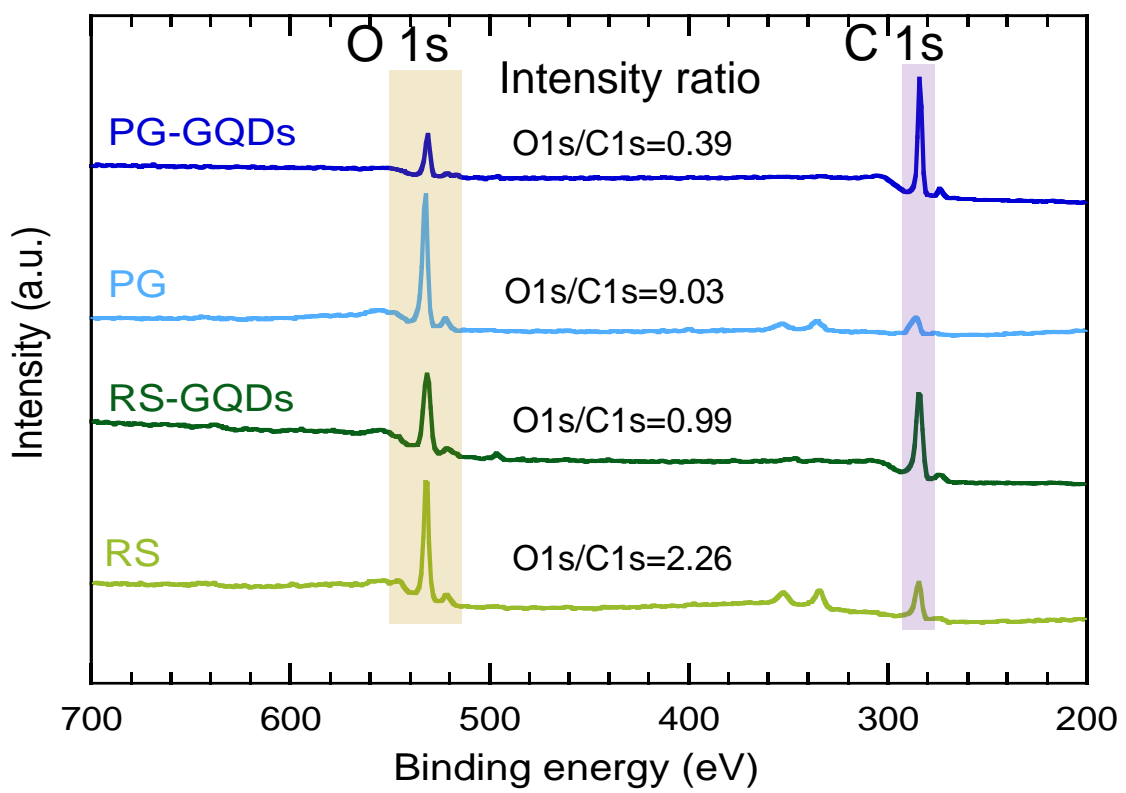


Fig. S16 Wide scan XPS spectra of PG, PG-GQDs, RS, and RS-GQDs.

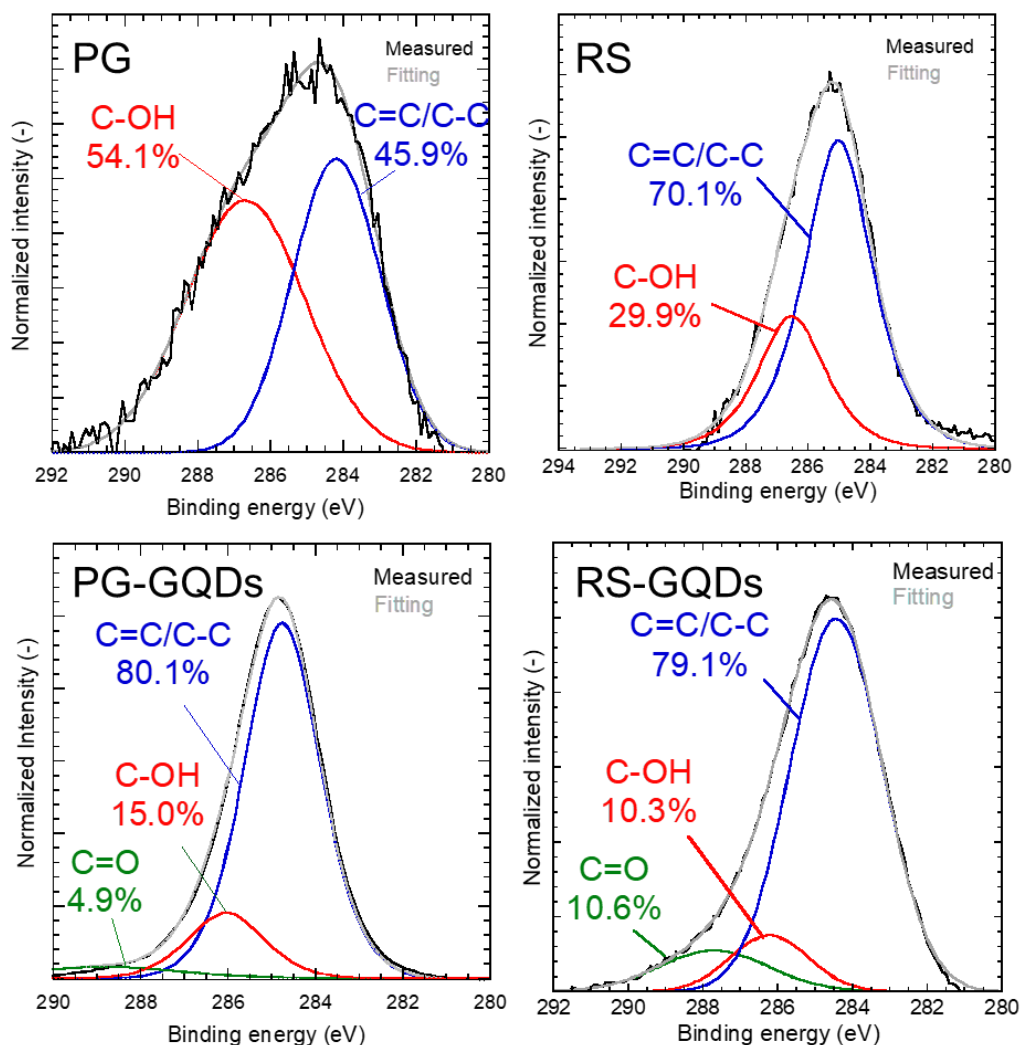


Fig. S17 Narrow scan C 1s XPS spectra of PG, PG-GQDs, RS, and RS-GQDs.

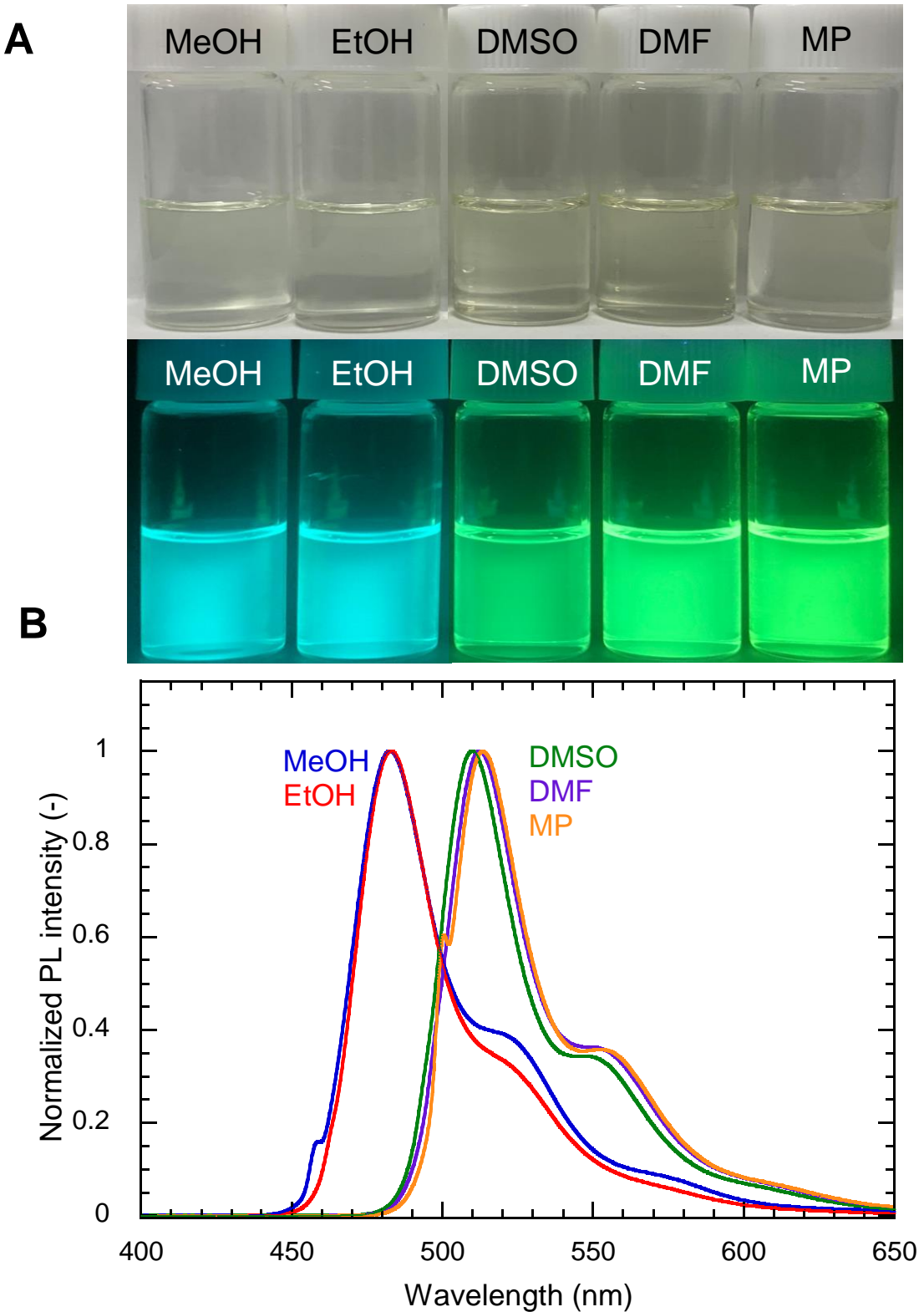


Fig. S18 (A) Photographs of purified PG-GQDs in solvents with different polarities under white light and 365 nm UV light and (B) their PL spectra.

Table S5 PL properties of purified PG-GQDs in solvents with different polarities.

| Dispersion | $E_T(30)$ (kcal mol ⁻¹) | λ_{ex} (nm) | λ_{em} (nm) | fw hm (nm) | PLQY (%) |
|---------------|--|---------------------|---------------------|------------|----------|
| MP | 42.2 | 500 | 514 | 33 | 96 |
| DMF | 43.2 | 498 | 513 | 32 | 94 |
| DMSO | 45.1 | 494 | 511 | 30 | 79 |
| EtOH | 51.9 | 463 | 484 | 32 | 80 |
| MeOH | 55.4 | 458 | 483 | 34 | 97 |
| Water (pH 7) | | 444 | 474 | 50 | 6 |
| Water (pH 9) | | 428 | 465 | 50 | 30 |
| Water (pH 11) | 63.1 | 428 | 465 | 49 | 60 |
| Water (pH 13) | | 428 | 466 | 49 | 52 |

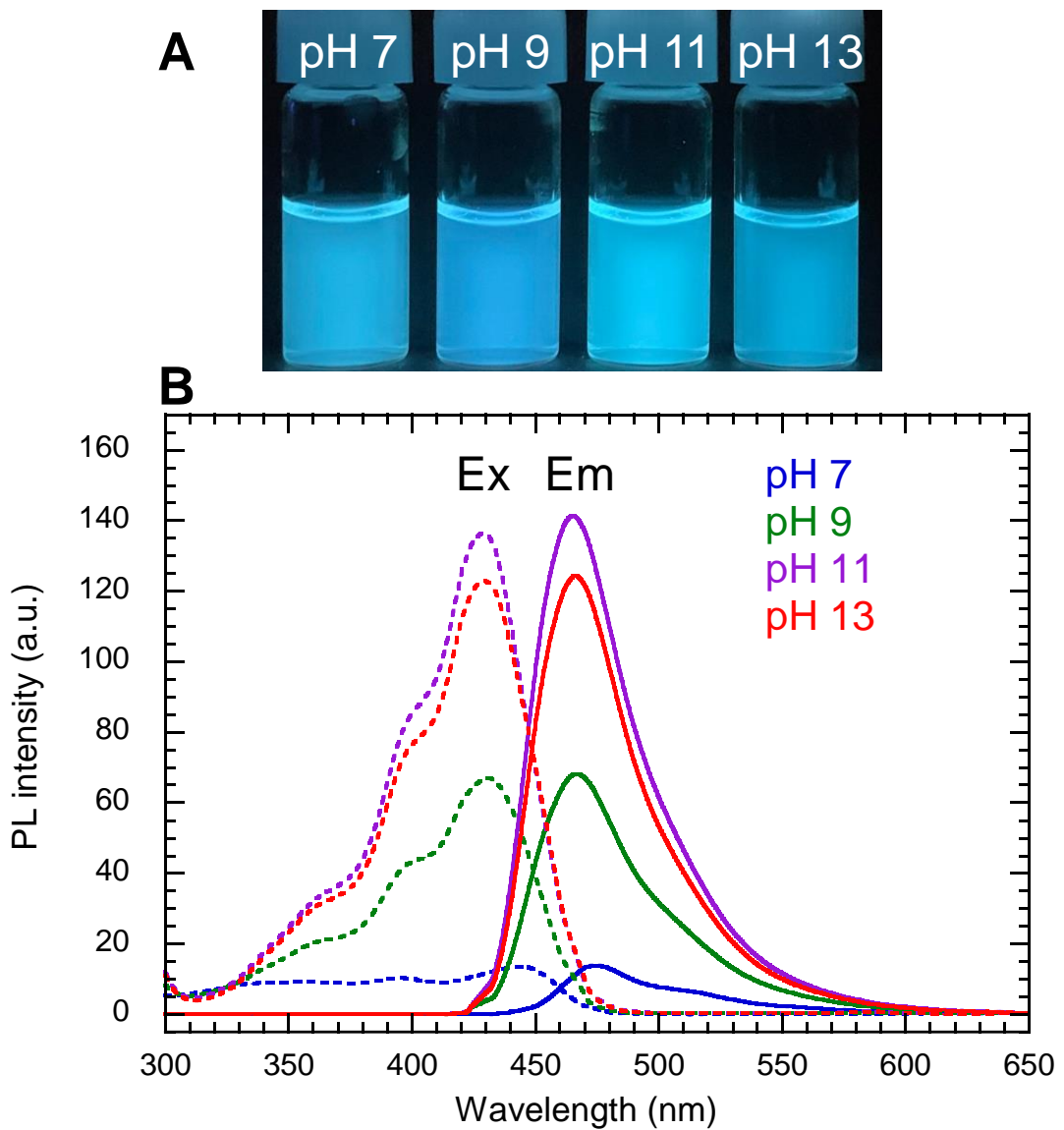


Fig. S19 (A) Photographs of purified PG-GQDs in water at different pH and (B) their PL/PLE spectra.

References

- S1 F. L. Yuan, T. Yuan, L. Z. Sui, Z. B. Wang, Z. F. Xi, Y. C. Li, X. H. Li, L. Z. Fan, Z. A. Tan and A. M. Chen, *Nat. Commun.*, 2018, **9**, 2249.
- S2 F. L. Yuan, P. He, Z. F. Xi, X. H. Li, Y. C. Li, H. Z. Zhong, L. Z. Fan and S. H. Yang, *Nano Res.*, 2019, **12**, 1669–1674.
- S3 S. Ghosh, H. Ali and N. R. Jana, *ACS Sustainable Chem. Eng.*, 2019, **7**, 12629–12637.